Journal of Gerontology: BIOLOGICAL SCIENCES
2008, Vol. 63A, No. 1, 3–11

Progressive Diastolic Dysfunction in the Female mRen(2).Lewis Rat: Influence of Salt and Ovarian Hormones

Leanne Groban,[1] Liliya M. Yamaleyeva,[2] Brian M. Westwood,[2] Timothy T. Houle,[1] Marina Lin,[1] Dalane W. Kitzman,[3] and Mark C. Chappell[2]

[1]Department of Anesthesiology, [2]Hypertension and Vascular Disease Center, and [3]Department of Cardiology, Wake Forest University School of Medicine, Winston-Salem, North Carolina.

This study determined the contribution of chronic salt loading and early loss of ovarian hormones on diastolic function in the hypertensive female mRen(2).Lewis rat, a monogenetic strain that expresses the mouse renin-2 gene in various tissues. Estrogen-intact mRen2 rats fed a high salt (HS) (8% sodium chloride) diet exhibited early diastolic dysfunction when compared to normal salt-fed (NS) (1% sodium chloride) rats. In contrast, ovariectomized (OVX) rats on either NS or HS diets showed impaired relaxation with evidence of elevated left ventricular filling pressures (E/e′) or pseudonormalization. This more advanced stage of diastolic dysfunction was associated with increases in interstitial cardiac fibrosis and high circulating levels of aldosterone, two factors leading to reduced ventricular compliance. These findings may explain the preponderance of diastolic dysfunction and diastolic heart failure in postmenopausal women and provide a potential animal model for evaluating prevention and treatment interventions for this disorder.

Key Words: Salt—Hormone, ovarian—Diastolic function—Rat.

THE relationship between hypertension and chronic heart failure is well established (1), and the importance of both the prevention and progression of left ventricular (LV) remodeling associated with hypertensive heart syndrome has been highlighted (2). However, despite its high prevalence among aging women (3,4), diastolic heart failure has received little attention in comparison to the heart failure that is common among middle-aged men, or systolic heart failure (2,5). One potential reason for the paucity of information in this rising sector of the population may be the controversy of recent clinical trials regarding the role of estrogen in older women with heart disease (6–8). Nonetheless, data suggest that women develop high blood pressure, especially systolic hypertension, at an increased rate as they age (9,10). Furthermore, it has been noted that women develop salt sensitivity and LV hypertrophy, particularly after menopause (11–15). Given these findings and the sexually dimorphic pattern of heart failure (5,16,17), it is reasonable to suspect that the loss of ovarian hormones associated with menopause or the surgical removal of ovaries is an important risk factor for diastolic dysfunction, the precursor of diastolic heart failure. It is unclear, however, to what extent changes in diastolic function and consequent risk of diastolic heart failure after menopause represent hormonal changes versus merely advancing age alone. Accordingly, appropriate experimental models are necessary to advance our understanding of ovarian hormone withdrawal on the development of hypertension, salt sensitivity, LV remodeling, and diastolic dysfunction, as well as provide insight into potential therapeutic approaches.

The aims of the current study were to evaluate the effects of ovarian hormone withdrawal and chronic salt loading on the development of diastolic dysfunction using the female mRen(2).Lewis (mRen2) rat, a monogenetic strain that expresses the mouse renin-2 gene in various tissues. This model is unique in that estrogen depletion by oophorectomy markedly exacerbates the development and maintenance of hypertension under normal salt conditions that appears dependent on an activated renin–angiotensin–aldosterone system (RAAS) (18–20). Moreover, the female mRen2 is sensitive to a high-salt (HS) diet, developing increased blood pressure, LV hypertrophy, and renal injury (19), clinical factors that strongly associate with diastolic dysfunction of aging. Accordingly, we hypothesized that the hypertensive, ovariectomized (OVX)-mRen2s on a normal-salt (NS) diet would show abnormalities in diastolic function similar to those observed in the salt-loaded, estrogen-intact mRen2.

Methods

All experimental procedures were designed in accordance with the protocols of the Institutional Animal Care and Use Committee of Wake Forest University School of Medicine and the Guide for the Care and Use of Laboratory Animals published by the National Institutes of Health (NIH Publication No 85-23, revised 1996).

Animal Model and Protocol

Hemizygous female mRen2s were obtained from the Hypertension and Vascular Disease Center Transgenic

colony. At 4 weeks of age, animals underwent either bilateral oophorectomy or were left intact. Between 5 and 15 weeks of age, animals were fed either a 1% (NS) or 8% (HS) ad libitum sodium chloride diet (Harlan TEKLAB, Madison WI). Rats were housed in metabolic cages (Harvard Bioscience, South Natick, MA) for assessment of food and water intake and urine collection for biochemical analysis. The Association for Assessment and Accreditation of Laboratory Animal Care (AALAC)-approved facility was maintained on a 12-hour light/dark cycle at constant temperature and humidity. Systolic blood pressure was measured at weekly intervals in trained rats (mean of five determinations per data point) with a Narco Biosystems device (Houston, TX). At the end of the study, transthoracic echocardiographic examinations were performed on anesthetized rats (ketamine HCL 60 mg/kg and xylazine HCL 5 mg/kg, intramuscular) by an experienced echocardiographer (L. Groban) masked to the treatment protocol. Immediately following the echocardiogram, anesthetized animals were killed by decapitation, trunk blood was collected, and hearts were rapidly removed, weighed, and stored for analysis. The cardiac weight index was expressed as mg heart weight/g total body weight. All animals were examined for the presence or absence of ovaries.

Echocardiographic Studies

Sedated, spontaneously breathing animals were placed in a shallow left lateral decubitus position with electrocardiographic adhesive electrodes applied to the paws. The left hemithorax was shaved and prepped with acoustic coupling gel to increase probe contact. Animals were secured to a warming table to maintain normothermia. Using a commercially available sector scanner equipped with a 12 MHz phased-array transducer (Envisor; Philips Medical Systems, Andover, MA), images were obtained at 100 mm/s sweep speed and recorded on a digital storage optical disc for offline analysis. LV M-mode images were obtained in the two-dimensional short axis view close to the papillary muscles. Diastolic posterior and anterior wall thicknesses at end diastole (PWTed, AWTed) and LV end-diastolic and end-systolic dimensions (LVDD, LVSD) were measured according to the American Society for Echocardiography leading-edge method (21). The percentage of LV fractional shortening (%FS), an index of global systolic function, was calculated as ((LVDD − LVSD)/LVDD) × 100. Mitral inflow measurements of early and late filling velocities (E_{max} and A_{max}, respectively), deceleration slope (E_{dec} slope), isovolumic relaxation time (IVRT), and early deceleration time ($E_{dectime}$) were obtained using pulsed Doppler, with the sample volume placed at the tips of mitral leaflets from an apical four-chamber orientation. Doppler tissue imaging to assess mitral valve septal annular velocities (e′) was also obtained from the four-chamber view. All measured and calculated systolic and diastolic indices are represented as the average of at least five consecutive cardiac cycles to minimize beat-to-beat variability.

Tissue Collection and Morphometric Measurements

After the whole heart was weighed, the atria were separated and the right ventricle was removed by cutting along its attachment to the left ventricle and septum. The left ventricle and septum were weighed as a single unit. A coronal section, taken from base to apex, through the left ventricle and papillary muscle was formalin fixed.

Heart specimens were dehydrated with ethanol and embedded in paraffin. Following microtome sectioning, the 4 μm tissue preparations underwent hematoxylin–eosin, Masson's Trichrome, and Verhoeff–van Gieson (VVG) staining for assessment of collagen and elastin fibers. Images of the LV free wall were taken at 10× objective using a Zeiss AxioCam digital camera and AxioVision software (Zeiss, Munchen-Hallbergmoos, Germany) by an observer who had no knowledge of treatment groups and previous results. Using Adobe Photoshop, a uniform series of image processing techniques were applied to a copy of each image to maximize the color differential between collagen and cardiac tissue. Color thresholding was used to select both the total amount of cardiac tissue and the total amount of collagen within each image. Given the intensity of the VVG staining as compared to the trichrome staining and the knowledge that collagen fibers traverse with elastin, the percent area of VVG-stained fibers for each image was calculated and used as an indicator of myocardial collagen.

Biochemical Analysis

Serum aldosterone levels were measured by a radioimmunoassay (RIA) kit (DPC, Los Angeles, CA) and expressed as ng/dL. To confirm the absence of ovaries, plasma estradiol levels were measured by an RIA kit (Polymedco, Inc., Cortlandt Manor, NY) and expressed as pg/mL. Values at or below the detectable level were arbitrarily assigned the detectable level of 5 mg/mL for statistical analysis.

Statistical Analysis

All analyses were conducted on SPSS (SPSS, Inc., Chicago, IL). Prior to performing the analyses, histograms and descriptive statistics were computed to confirm the assumptions needed for parametric analysis. A log transformation of collagen scores was used to better achieve a normal distribution.

To reduce the number of conducted significance tests, the ''echo data'' were combined into meaningful subsets using principal components analysis (factor analysis). This well-established technique examines the correlations among the variables and uses these relationships to reduce the number of observed variables to a smaller number of reliable subsets (22,23) and to avoid Type I error inflation. The factor analysis reduced the original set of 13 variables down to five composite variables while still representing 91% of the original variance. The solution appeared to represent the original variables well (i.e., most factor loadings exceeded .80) and was clinically coherent. A Varimax rotation was used with unit scoring to combine the measurements into five composite dependent variables as follows:

1. e′ factor = e′ − E/e′
2. A factor = E/A − A_{max}
3. Wall thickness factor = LVDD(M-mode) − Pwted − Awted

Table 1. Systolic Blood Pressure, Body Weight, and Postmortem Heart Weights of the Four Experimental Groups

			Estrogen		Salt		Interaction	
Variables	Normal Salt	High Salt	p Value	η^2	p Value	η^2	p Value	η^2
Systolic blood pressure (mmHg)								
Intact	142 ± 7	206 ± 5	.008	0.29	.00001	0.753	.195	0.079
OVX	171 ± 5	217 ± 9						
Body weight (g)								
Intact	266 ± 6	220 ± 6	.0001	0.647	.0001	0.728	.798	0.005
OVX	300 ± 5	258 ± 5						
Whole heart weight (g)								
Intact	.862 ± .04	1.136 ± .02	.032	0.202	.0001	0.668	.257	0.061
OVX	.986 ± .04	1.177 ± .04						
Heart/Body weight (mg/g)								
Intact	3.24 ± .12	5.16 ± .08	.051	0.169	.0001	0.879	.025	0.217
OVX	3.29 ± .11	4.58 ± .17						

Notes: Data represent mean ± standard error of the mean.
OVX = ovariectomized.

4. Systolic factor = LVSD − FS
5. E factor = E_{dec} time + IVRT − E_{max} − E_{dec} slope.

Two multivariate analyses of variance (MANOVAs) were conducted, one with the five dependent variables (''echo data'' factors), the other with two dependent variables (aldosterone and blood pressure). For these comparisons, α was determined by dividing .05 (the desired comparison-wise error rate) by the number of dependent variables (resulting in $\alpha = .01, .025$). An additional three ANOVAs were conducted on collagen, heart weight/body weight, and plasma estradiol. All comparisons examined estrogen (intact vs OVX) and salt (Level 1 vs Level 2) and Estrogen × Salt interaction as between-subject factors.

To better index the effect size induced by each of the factors, partial η^2, a measure of the proportion of variance in the dependent variable accounted for by the factor, is also reported. Although rules of thumb concerning the interpretation of effect size measures can be problematic (24), 10% of the variance is commonly considered to be a ''small'' effect ($\eta^2 = .10$), 25% of the variance is a ''medium'' effect ($\eta^2 = .25$), and 40% or greater is considered a ''large'' effect ($\eta^2 \geq .40$) (24).

Results

Blood Pressure, Body Weight, and Heart Weight

Blood pressure, body weight, and heart weights are shown in Table 1. Consistent with our previous studies (18–20), ovariectomy at 4 weeks of age significantly increased blood pressure in the mRen2 at 15 weeks of age. Specifically, estrogen, irrespective of salt, accounted for 29% of the variance in blood pressure among groups. Likewise, HS had a significant effect on elevating blood pressure such that its presence alone accounted for 75% of the variance in blood pressure. The OVX-HS rats exhibited the highest blood pressure among groups, although these values were not statistically different from Intact-HS rats ($p = .195$, $\eta^2 = .079$). Body weight was significantly increased in OVX rats compared to their respective NS and HS cohorts (Estrogen: $F(1,21) = 38.54$, $p = .000$, $\eta^2 = .647$; Salt: $F(1,21) = 56.14$, $p = .000$, $\eta^2 = .728$). The heart weight-to-body weight ratios were highest in the Intact-HS and OVX-HS animals. Interestingly, the normalized heart weight in the OVX-NS group was not different from Intact-NS rats, despite exacerbated hypertension following oophorectomy which is consistent with our previous report (19). As expected, plasma estradiol levels were greater in intact versus OVX rats (24 ± 6 mg/mL vs 5 ± 0 pg/mL).

Echocardiography

M-mode.—Echocardiography was successful in every case. Within-observer reproducibility values for %FS, Pwted, E_{max}, A_{max}, and e′ were 8 ± 1%, 6 ± 1%, 7 ± 2%, 16 ± 4%, and 8 ± 4, respectively. M-mode measurements of LV dimensions, systolic function, and wall thicknesses are summarized in Table 2. No differences in LVSD or %FS were apparent with respect to estrogen or salt (Table 2). The wall thickness factor, comprising M-mode measurements of PWTed and AWTed and LVDD, was significantly increased amid estrogen deficiency or the presence of HS. In fact, up to 40% of the variance in wall thickness can be attributed to either one of these treatments. Although heart rates during anesthesia (in beats per minute: Intact-NS: 242 ± 14; OVX-NS: 216 ± 15; Intact-HS; 249 ± 8; OVX-HS: 231 ± 11) were only 15% lower than that reported previously in the same animal model during conscious conditions (19), heart rates were significantly higher in Intact-HS versus OVX-NS mRen2s in the present study.

Doppler.—In contrast to systolic function, the presence of HS and loss of estrogen, independently and additively, impaired diastolic function as assessed by Doppler transmitral flow and tissue imaging. Using both Doppler modalities, the spectrum of diastolic dysfunction, e.g., normal, delayed relaxation, and delayed relaxation with high filling pressures or pseudonormalization, was expressed in the female mRen2 (Figure 1). As shown in Table 2, E/A was lowest in the Intact-HS group, whereas LV end diastolic pressures,

Table 2. Echocardiographic Characteristics of the Four Experimental Groups

	Normal Salt		High Salt		Estrogen		Salt		Interaction	
Variable	Intact	OVX	Intact	OVX	*p* Value	η^2	*p* Value	η^2	*p* Value	η^2
e′ factor					*.001*	*.43*	*.56*	*.02*	*.58*	*.01*
e′ (cm/s)	3.01 ± .29	1.92 ± .16	2.15 ± .09	1.85 ± .18	.002	.36				
E/e′	22 ± 2	30 ± 2	24 ± 2	30 ± 2	.001	.43				
A factor					*.01*	*.27*	*.02*	*.23*	*.17*	*.09*
E/A	2.06 ± .16	2.09 ± .19	1.12 ± .11	1.81 ± .20	.06	.16	.005	.32		
A_{max} (cm/s)	34 ± 4	29 ± 2	47 ± 3	32 ± 3	.011	.27	.025	.22		
Wall thickness factor					*.001*	*.40*	*.001*	*.41*	*.51*	*.02*
LVEDD (cm)	.64 ± .23	.62 ± .20	.65 ± .21	.58 ± .20	.03	.20	.41	.03		
PWTed (cm)	.21 ± .01	.26 ± .01	.26 ± .01	.32 ± .01	.001	.47	.001	.52		
AWTed (cm)	.20 ± .01	.24 ± .01	.26 ± .01	.29 ± .00	.001	.44	.001	.74		
Systolic factor					*.68*	*.01*	*.51*	*.02*	*.82*	*.003*
LVESD (cm)	.37 ± .23	.35 ± .20	.35 ± .21	.34 ± .20						
%FS	43 ± 2	43 ± 2	47 ± 2	41 ± 2						
E factor					*.32*	*.05*	*.007*	*.30*	*.05*	*.17*
E_{dec} time (s)	0.046 ± .002	0.05 ± .002	0.046 ± .002	0.048 ± .002			.78	.00		
IVRT (s)	0.025 ± .000	0.031 ± .0001	0.031 ± 0.002	0.035 ± .002			.01	.28		
E_{max} (cm/s)	65 ± 3	57 ± 2	51 ± 3	54 ± 2			.004	.33		
E_{dec} slope (cm/s^2)	14 ± 1	11 ± 1	11 ± 1	11 ± 1			.12	.11		

Notes: Data represent mean ± standard error of the mean. Variables in italics represent the five factors as determined from the Varimax analysis. The individual echocardiographic variables corresponding to each factor are listed with significance data when the overall factor is significant.

OVX = ovariectomized; e′ = early mitral annular velocity; E/e′ = early transmitral filling velocity-to-mitral annular velocity; E/A = early-to-late transmitral filling ratio; E_{max} = maximum early transmitral filling velocity; A_{max} = maximum late transmitral filling velocity; LVEDD = left ventricular end diastolic dimension; PWTed = posterior wall thickness at end diastole; AWTed = anterior wall thickness at end diastole; LVESD = left ventricular end systolic dimension; %FS = percent fractional shortening; E_{dec} time = early deceleration time; IVRT = isovolumic relaxation time; E_{dec} slope = early deceleration slope.

reflected via E/e′ (Figure 2), were relatively unchanged from that of the NS cohort. This lower E/A ratio in Intact-HS rats appeared to be a function of a 22% reduction in early filling velocity of the left ventricle (E_{max}) across the mitral valve and a 43% increase in late filling velocity (A_{max}) compared to Intact-NS rats, indicating a greater fraction of LV filling in late diastole; otherwise known as early or mild diastolic dysfunction (25) (Table 2). Interestingly, in the OVX rats (both NS and HS groups), the E/A ratios were similar whereas LV filling pressures (E/e′) were significantly greater than that of the estrogen-intact, NS-fed rats. Estrogen, irrespective of salt, accounted for 43% of the variance in the E factor (E/e′ and e′). Taken together, these findings indicate that (a) mild diastolic dysfunction is present in Intact-HS mRen2s; (b) early estrogen depletion (at 4 weeks of age) under NS conditions intensifies diastolic dysfunction, indicated by delayed relaxation (lower e′ relative to Intact rats) and increased filling pressures, also called transmitral pseudonormalization; and (c) estrogen depletion and HS have additive, unfavorable effects on diastolic function, also exhibiting pseudonormalization.

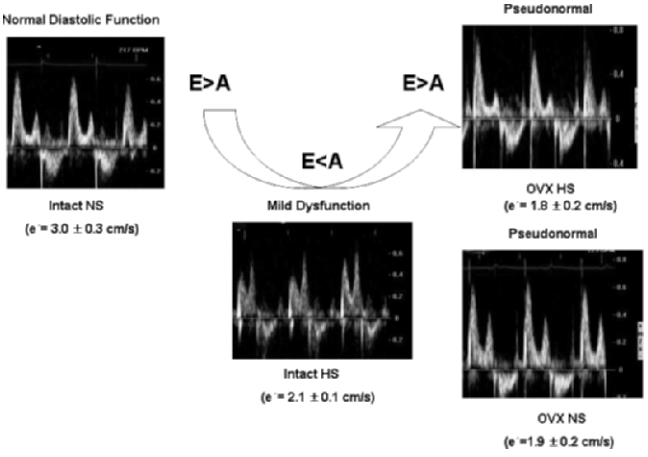

Figure 1. Progression of diastolic dysfunction in the female mRen(2).Lewis (mRen2) rat with salt loading and ovariectomy (OVX). Intact-normal salt (NS) mRen2 rats show normal diastolic function manifested by E/A ratio >1 and e′ = 3.0 ± 0.3 cm/s. Intact-high salt (HS) mRen2 rats show mild diastolic dysfunction manifested by E/A ratio < 1 and low e′ relative to that of Intact-NS mRen2 rats. OVX-NS and -HS mRen2 rats show pseudonormal patterns of diastolic function manifested by E/A ratios > 1 and relatively low e′ velocities compared to Intact-NS rats. E = early transmitral filling velocity; A = late transmitral filling velocity; e′ = early mitral annular descent (septal) velocity.

Histopathology

LV interstitial collagen was most pronounced in the OVX-HS rats as compared to estrogen-intact rats on NS and HS diets (Figure 3A and B). Interestingly, estrogen, irrespective of salt, contributed to 40% of the variance in interstitial collagen whereas salt alone contributed to 15% of the variance in LV remodeling. The combination of estrogen deficiency and HS tended to have a synergistic effect on LV remodeling, accounting for 12% of the variance in interstitial collagen ($p = .136$, $\eta^2 = .119$).

Serum Aldosterone

Given the association between mineralocorticoids, salt-sensitive hypertension, and cardiac fibrosis (26,27), we determined serum aldosterone as a marker of mineralocorticoid

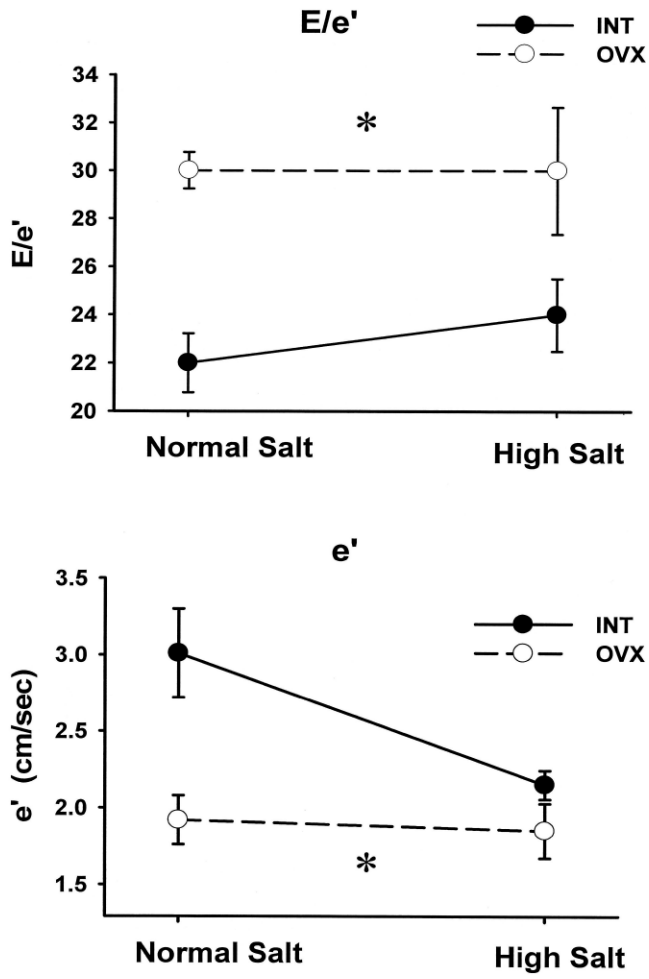

Figure 2. Influence of ovariectomy (OVX) and a high salt diet on tissue doppler factor values. Mitral annular descent (e′) and left ventricular (LV) filling pressure (E/e′). Data represent mean and standard error of the mean. *$p < .025$ for estrogen effect. é Factor (including é, E/é), estrogen: F(1,21) = 16.13, $p = .001$, $\eta^2 = .43$. INT = intact.

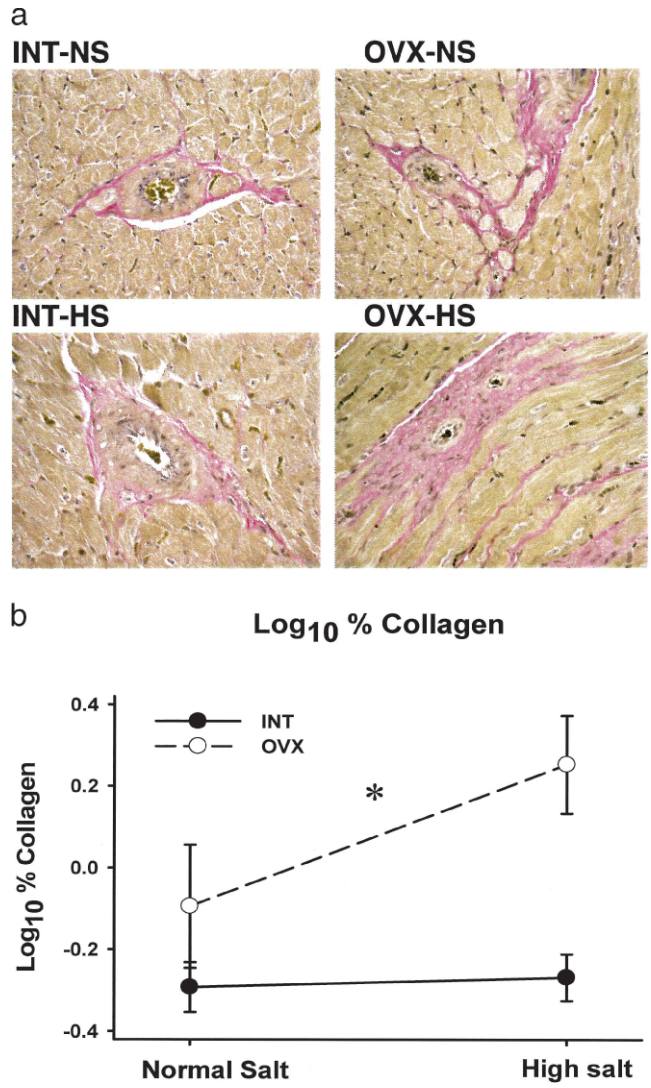

Figure 3. **A,** Representative images of the left ventricular free wall interstitial collagen were taken at a magnification of 40×. Following VVG (Verhoeff–van Gieson) staining, *red* areas represent interstitial collagen. The VVG-stained slides revealed that the ovariectomized-high salt (OVX-HS) group had the highest amount of collagen followed by the OVX-normal salt (NS), Intact (INT)-HS, and INT-NS groups. **B,** Data represent mean ± standard error of the mean. *$p < .025$ for estrogen effect. Log_{10} % collagen, Estrogen: F(1,18) = 12.02, $p = .003$, $\eta^2 = .400$; Salt: F(1,18) = 3.22, $p = .09$, $\eta^2 = .152$; Estrogen + Salt: F(1,18) = 2.43, $p = .136$, $\eta^2 = .119$.

activity in the mRen2 groups. Circulating aldosterone was suppressed in the presence of HS, and this treatment attributed to 28% of the variance in mineralocorticoid levels among groups. Serum aldosterone levels were greatest in OVX-NS as compared to Intact-NS and OVX-HS rats. Although the increase in serum aldosterone of the estrogen-depleted rats did not reach statistical significance ($F = 5.87$, $p = .025$), estrogen depletion accounted for 22% of the variance in aldosterone levels among groups (Figure 4).

Discussion

These studies are the first demonstration by echocardiography of the additive effects of estrogen depletion and HS intake on the progressive decrement in diastolic function in the female mRen2 strain. We have shown that the female mRen2 exhibits both estrogen and salt sensitivity on the development and progression of high blood pressure and renal injury that is dependent on an activated RAAS (18,19). Indeed, the AT1 receptor antagonist olmesartan lowered blood pressure to the same extent as exogenous β-estradiol in the OVX mRen2 (18).

The present results show that Intact-HS mRen2 females exhibit impaired LV filling as evidenced by reduced E/A ratios and early-wave mitral annular velocities (e′). OVX rats on NS and HS diets also showed impaired relaxation, or reduced e′; however, the E/A ratios and LV filling pressures (defined by E/e′) were higher than those of Intact-NS rats, suggesting that estrogen depletion exacerbated diastolic dysfunction to a greater extent than salt alone. In addition, this impaired LV filling and presumed increase in LV stiffness in the OVX mRen2 was associated with increased

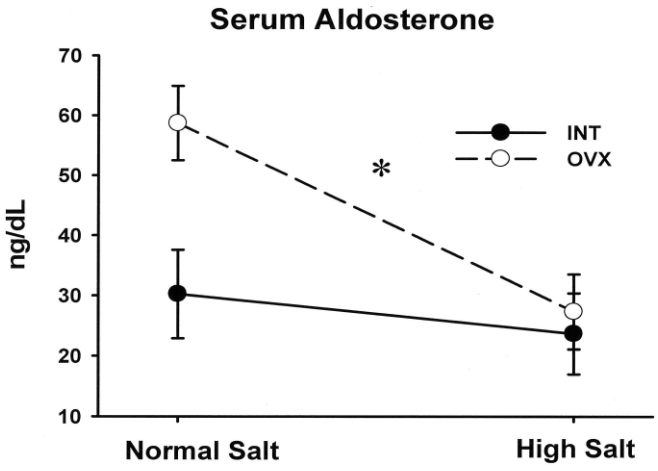

Figure 4. The effect of ovariectomy (OVX) and a high-salt diet on serum aldosterone levels in the female mRen(2).Lewis (mRen2) rats. Data represent mean ± standard error of the mean. $^{\dagger}p < .025$ for salt effect. Estrogen: $F(1,21) = 5.87$, $p = .025$, $\eta^2 = .219$; Salt: $F(1,21) = 8.20$, $p = .009$, $\eta^2 = .281$; Estrogen + Salt: $F(1,21) = 3.50$, $p = .075$, $\eta^2 = .143$. INT = intact.

interstitial cardiac fibrosis and higher circulating levels of aldosterone, a potent profibrotic mineralocorticoid (26,27).

The mild or *early* diastolic dysfunction observed in the Intact-HS mRen2 is exemplified by a greater fraction of LV filling in *late* diastole (increased A velocity). This condition may be related to the pronounced increase in systemic blood pressure (>60 mmHg) and compensatory LV hypertrophy (increased heart weight-to-body weight ratio and LV wall thickness) as a consequence of the HS diet. Salt loading and the resultant high blood pressure are known to promote cardiac hypertrophy in both clinical and experimental studies (28–31). LV hypertrophy has also been linked to the source of early diastolic dysfunction (32,33). Likewise, reductions in E/A have been demonstrated in salt-sensitive patients with essential hypertension (34) and in salt-loaded, spontaneously hypertensive rats (SHR) that do not exhibit overt heart failure (28).

Salt intake clearly influences LV remodeling (11), and interstitial LV fibrosis interferes with ventricular relaxation (35). The mechanisms for reduced LV filling in the Intact-HS mRen2 remain unclear because cardiac interstitial collagen was only modestly increased. The degree of fibrosis in the mRen2 differs to some extent from other experimental models including the Wistar, Wistar-Kyoto, and SHR rats, in which high dietary salt produce LV hypertrophy (LVH) and profound increases in cardiac collagen (28,36,37). Differences in species, duration of salt loading, and age of the rats may account for some of these disparate findings. Alternatively, the attenuated LV remodeling with HS in the estrogen-intact mRen2 may reflect a protective role of ovarian hormones as the previous studies used only male rats. Estrogen increases nitric oxide synthase (NOS) activity (38) and expression of its various isoforms (39–41), which may contribute to the maintenance of cardiac architecture (42,43). Nitric oxide is suggested to mediate expression of cyclooxygenase-2, which has also been shown to be involved in cardioprotection (44,45). Moreover, both estrogen and progesterone reduce stimulated growth of cardiofibroblasts, suggesting that ovarian hormones may counterbalance salt-induced LV remodeling and the evolution of diastolic dysfunction in the Intact-HS mRen2 female (46).

Estrogen depletion accelerated the progression of diastolic dysfunction in the mRen2s. The normal mitral inflow pattern (E > A) and the reduced tissue Doppler mitral annular descent constitute a pseudonormal diastolic pattern. In addition, the increased E/e′ ratio implies that OVX animals required higher filling pressures during diastole than their respective intact cohorts, presumably due to increased myocardial stiffness. Given that pseudonormalization coincided with the appearance of increased cardiac fibrosis further suggests estrogen's potential role in the maintenance of cardiac architecture and diastolic function. Interstitial fibrosis can directly impede myocardial relaxation (35) as well as indirectly through reductions in diastolic coronary flow and myocardial perfusion (47). Hypertension itself also promotes cardiac fibrosis and LV stiffness (48); however, the diastolic filling abnormalities observed in the OVX-NS rats with exacerbated hypertension were independent of changes in LV size (heart weight-to-body weight ratios were similar to those of Intact-NS rats). As the elevated blood pressures were similar between the Intact- and OVX-HS rats whereas cardiac collagen was greatest in OVX-HS rats, these data suggest that LV remodeling and diastolic pseudonormalization were, to a certain extent, independent of hypertension. In this regard, the depletion of ovarian hormones may promote cardiac growth factors to induce fibrosis and, in turn, lead to reductions in myocardial distensibility and diastolic dysfunction (46).

Alternatively, early activation of the circulating RAAS in the OVX mRen2 may accelerate the progression of hypertensive heart disease (49). Loss of estrogen is known to result in increased expression of angiotensin-converting enzyme (ACE), AT1 receptors, and Ang II (18,50). In addition, female spontaneously hypertensive heart failure (SHHF) rats exhibit a delayed increase in plasma renin activity (51) compared to male SHHF rats, suggesting an estrogen-mediated attenuation of RAAS activation. Moreover, in aging female SHHF rats, elevated renin is apparent 3–6 months after the cessation of normal estrous cycling (51–53). Likewise, plasma renin activity increases to a greater extent in the male than in the female two-kidney-one-clip (2K1C) rats (52). Recent findings from Chappell and colleagues (18,19) also show that estrogen depletion in the female mRen2 disinhibits the circulating RAAS. These findings, taken together with the fact that aldosterone is associated with myocardial fibrosis in experimental studies (26,54) and sex-related differences in LV remodeling (55), imply that the elevated circulating levels of aldosterone observed in the OVX-NS mRen2 may have contributed to the increase in interstitial collagen observed in this group. Both estrogen and aldosterone receptors are present in cardiac fibroblasts and myocytes (56); thus, both hormones could have a role in modulating the cardiac interstitial matrix. Although circulating levels of aldosterone were suppressed in the OVX-HS group, aldosterone may be inappropriately high for the level of

salt and/or blood pressure. Interestingly, chronic salt loading is associated with increased cardiac aldosterone production. Takeda and colleagues (57) showed that administration of 0.9% salt to Wistar-Kyoto rats stimulated cardiac aldosterone synthetase activity, expression of aldosterone synthase genes, and aldosterone production in the heart. Increased levels of cardiac aldosterone and myocardial fibrosis in the absence of changes in plasma aldosterone were reported in Wistar rats following coronary ligation (54). Although cardiac tissue levels of aldosterone were not assessed in the present study, ovarian hormonal loss in the mRen2, in the presence or absence of salt loading, could contribute to LV remodeling and diastolic dysfunction via an exaggerated activation of the cardiac RAAS, particularly, aldosterone. Future studies will address whether the cardiac components of the RAAS including aldosterone, Ang II, and the antiproliferative metabolite Ang-(1-7), as well as their receptors (58), are altered in the mRen2 following estrogen depletion or increased sodium intake.

Our findings of increased circulating aldosterone with increased cardiac interstitial collagen and progressive diastolic dysfunction correspond to several animal studies that report regression of cardiac hypertrophy and fibrosis with aldosterone receptor antagonism (36). Indeed, data from a few pilot clinical studies support a benefit for aldosterone antagonism in the management of diastolic dysfunction and diastolic heart failure. In older women with diastolic dysfunction (59) or diastolic heart failure (60), spironolactone was well tolerated and appeared to improve diastolic function, exercise capacity, and quality of life. Moreover, Izawa and colleagues (61) showed that mineralocorticoid receptor antagonism ameliorated diastolic dysfunction, reduced chamber stiffness, and increased regression of myocardial fibrosis in mildly symptomatic patients with dilated cardiomyopathy. Although further delineation of the clinical role of aldosterone antagonism in the management of gender-specific diastolic heart failure requires the completion of the TOPCAT trial (www.topcatstudy.com/org.asp), our animal correlate provides a unique tool to gain a thorough understanding of the link between ovarian hormonal loss and aldosterone activity in the subsequent development of diastolic heart dysfunction.

Several limitations can be identified in this study. First, cardiac function was based on noninvasive evaluation of hemodynamics and myocardial performance. Thus, direct information on filling pressures and the decrease in LV isovolumetric pressure or its time constant τ are not available. However, our investigation was based on both transmitral and tissue Doppler echocardiography, which are the methods of choice for routine noninvasive evaluation of diastolic function in humans (62). Compared with conventional transmitral Doppler flow, tissue Doppler of the early diastolic velocity at the mitral annulus (e') is less influenced by loading conditions (63,64) and has been closely related to invasive measurements of diastolic function in humans and animals (65,66). Indeed, the increased heart rate in the Intact-HS mRen2 as compared to heart rates observed among the other treatments may have had a role in the reduced E/A ratio observed in this group. However, whereas ''late'' transmitral (or A wave) velocities vary as a function of heart rate, ''early'' (or E wave) transmitral and tissue Doppler velocities have been shown to be independent of heart rate (63,64,67,68). In addition, the ratio E/e' corrects for the influence of relaxation on transmitral E, regardless of heart rate (69), and it relates strongly to filling pressures in humans (64,70) and in rats (71). However, it remains unclear whether the standard cutoffs used in humans for elevated filling pressure apply to rats because an E/e' of 16 has been shown to correlate with an LV end diastolic pressure of 9 mmHg in normotensive Wistar rats (71) and $E/e' \geq 16$ correlates with filling pressures (pulmonary capillary wedge pressure) $\geq$20 mmHg in patients (69). Accordingly, in the present study, we used the Intact-NS mRen as our control, and any increase in E/e' relative to this treatment group was considered as ''elevated'' filling pressures.

All told, transmitral and tissue Doppler recordings from OVX-NS or -HS mRens are consistent with the diastolic pattern of delayed relaxation with high filling pressures, or pseudonormalization, whereas recordings taken from Intact-HS rats resemble an earlier stage of diastolic impairment whereby filling pressures are analogous to the control mRen2.

Despite epidemiological evidence that the incidence of diastolic heart failure in women increases as estrogen levels regress during menopause, and that salt sensitivity, hypertension, and diastolic dysfunction antedate the clinical manifestations of the disease, the pathophysiology and appropriate therapeutic approaches remain unknown. An important step in addressing this unmet public health need is the establishment of an animal correlate of estrogen-sensitive diastolic dysfunction. Accordingly, the present study reveals that the female mRen2 strain, a monogenetic rat model of tissue renin expression and angiotensin II-dependent hypertension, is an estrogen- and salt-sensitive model of diastolic dysfunction. Moreover, the body weight differences between OVX and estrogen-intact rats may contribute, in part, to diastolic dysfunction given the clinical association of obesity with LV remodeling and diastolic dysfunction in patients without coronary artery disease (72).

Conclusion

This new congenic model may allow for the greater elucidation of the mechanisms and potential treatments associated with estrogen- and salt-sensitive diastolic dysfunction.

Acknowledgments

These studies were supported in part by grants from Dennis Jahnigen Career Development (LG); by National Institutes of Health grants KO8-AG026764-02 Paul Beeson award (LG), HL-56973 (MCC), HL-51952 (MCC), P60AG10484 (DWK), and R37 AG18915 (DWK); and by American Heart Association grants AH-151521 (MMC) and AHA-355741 (LMY). An unrestricted grant from the Unifi Corporation (Greensboro, NC) and the Farley–Hudson Foundation (Jacksonville, NC) is also acknowledged.

Correspondence

Address correspondence to Leanne Groban, MD, Department of Anesthesiology, Wake Forest University School of Medicine, Medical Center Blvd., Winston-Salem, NC 27127-1009. E-mail: lgroban@wfubmc.edu

References

1. Levy D, Larson MG, Vasan RS, Kannel WB, Ho KK. The progression from hypertension to congestive heart failure. *JAMA*. 1996;275:1557–1562.
2. Hunt SA, Abraham WT, Chin MH, et al., American College of Cardiology; American Heart Association Task Force on Practice Guidelines; American College of Chest Physicians; International Society for Heart and Lung Transplantation; Heart Rhythm Society. ACC/AHA 2005 Guideline Update for the Diagnosis and Management of Chronic Heart Failure in the Adult: a report of the American College of Cardiology/American Heart Association Task Force on Practice Guidelines (Writing Committee to Update the 2001 Guidelines for the Evaluation and Management of Heart Failure): developed in collaboration with the American College of Chest Physicians and the International Society for Heart and Lung Transplantation: endorsed by the Heart Rhythm Society. *Circulation*. 2005;112:e154–e235.
3. Kitzman DW, Gardin JM, Gottdiener JS, et al., Cardiovascular Health Study Research Group. Importance of heart failure with preserved systolic function in patients > or = 65 years of age. CHS Research Group. Cardiovascular Health Study. *Am J Cardiol*. 2001;87:413–419.
4. Masoudi FA, Havranek EP, Smith G, et al. Gender, age, and heart failure with preserved left ventricular systolic function. *J Am Coll Cardiol*. 2003;41:217–223.
5. Kitzman DW, Little WC, Brubaker PH, et al. Pathophysiological characterization of isolated diastolic heart failure in comparison to systolic heart failure. *JAMA*. 2002;288:2144–2150.
6. Grady D, Herrington D, Bittner V, et al., HERS Research Group. Cardiovascular disease outcomes during 6.8 years of hormone therapy: Heart and Estrogen/progestin Replacement Study follow-up (HERS II). *JAMA*. 2002;288:49–57.
7. Hulley S, Grady D, Bush T, et al. Randomized trial of estrogen plus progestin for secondary prevention of coronary heart disease in postmenopausal women. Heart and Estrogen/progestin Replacement Study (HERS) Research Group. *JAMA*. 1998;280:605–613.
8. Rossouw JE, Anderson GL, Prentice RL, et al., Writing Group for the Women's Health Initiative Investigators. Risks and benefits of estrogen plus progestin in healthy postmenopausal women: principal results from the Women's Health Initiative randomized controlled trial. *JAMA*. 2002;288:321–333.
9. Gheorghiade M, Abraham WT, Albert NM, et al., OPTIMIZE-HF Investigators and Coordinators. Systolic blood pressure at admission, clinical characteristics, and outcomes in patients hospitalized with acute heart failure. *JAMA*. 2006;296:2217–2226.
10. Hajjar I, Kotchen TA. Trends in prevalence, awareness, treatment, and control of hypertension in the United States, 1988–2000. *JAMA*. 2003;290:199–206.
11. Heimann JC, Drumond S, Alves AT, Barbato AJ, Dichtchekenian V, Marcondes M. Left ventricular hypertrophy is more marked in salt-sensitive than in salt-resistant hypertensive patients. *J Cardiovasc Pharmacol*. 1991;17(Suppl 2):S122–S124.
12. Pechere-Bertschi A, Burnier M. Female sex hormones, salt, and blood pressure regulation. *Am J Hypertens*. 2004;17:994–1001.
13. Schulman IH, Aranda P, Raij L, Veronesi M, Aranda FJ, Martin R. Surgical menopause increases salt sensitivity of blood pressure. *Hypertension*. 2006;47:1168–1174.
14. Weinberger MH. Salt sensitivity as a predictor of hypertension. *Am J Hypertens*. 1991;4:615S–616S.
15. Weinberger MH. Estrogens, salt, blood pressure, and cardiovascular disease in women: how do we interpret the data? *Hypertension*. 2006;47:1049–1050.
16. Bella JN, Palmieri V, Kitzman DW, et al. Gender difference in diastolic function in hypertension (the HyperGEN study). *Am J Cardiol*. 2002;89:1052–1056.
17. Ceia F, Fonseca C, Mota T, et al., EPICA Investigators. Prevalence of chronic heart failure in Southwestern Europe: the EPICA study. *Eur J Heart Fail*. 2002;4:531–539.
18. Chappell MC, Gallagher PE, Averill DB, Ferrario CM, Brosnihan KB. Estrogen or the AT1 antagonist olmesartan reverses the development of profound hypertension in the congenic mRen2.Lewis rat. *Hypertension*. 2003;42:781–786.
19. Chappell MC, Yamaleyeva LM, Westwood BM. Estrogen and salt sensitivity in the female mRen(2).Lewis rat. *Am J Physiol Regul Integr Comp Physiol*. 2006;291:R1557–R1563.
20. Yamaleyeva LM, Gallagher PE, Vinsant S, Chappell MC. Discoordinate regulation of renal nitric oxide synthase isoforms in ovariectomized mRen2.Lewis rats. *Am J Physiol Regul Integr Comp Physiol*. 2007;292:R819–R826.
21. Sahn DJ, DeMaria A, Kisslo J, Weyman A. Recommendations regarding quantitation in M-mode echocardiography: results of a survey of echocardiographic measurements. *Circulation*. 1978;58:1072–1083.
22. Harrell FE. *Regression Modeling Strategies: With Applications to Linear Models, Logistic Regression, and Survival Analysis*. New York: Springer; 2001.
23. Tabachnick BG, Fedell LS. *Using Multivariate Statistics,* 4th Ed. Needham Heights, MA: Allyn & Bacon; 2001.
24. Cohen J. *Statistical Power Analysis for the Behavioral Sciences,* 2nd Ed. Mahwah, NJ: Lawrence Erlbaum; 1988.
25. Rakowski H, Appleton C, Chan KL, et al. Canadian consensus recommendations for the measurement and reporting of diastolic dysfunction by echocardiography: from the Investigators of Consensus on Diastolic Dysfunction by Echocardiography. *J Am Soc Echocardiogr*. 1996;9:736–760.
26. Brilla CG, Zhou G, Matsubara L, Weber KT. Collagen metabolism in cultured adult rat cardiac fibroblasts: response to angiotensin II and aldosterone. *J Mol Cell Cardiol*. 1994;26:809–820.
27. Young MJ, Funder JW. Mineralocorticoids, salt, hypertension: effects on the heart. *Steroids*. 1996;61:233–235.
28. Ahn J, Varagic J, Slama M, Susic D, Frohlich ED. Cardiac structural and functional responses to salt loading in SHR. *Am J Physiol Heart Circ Physiol*. 2004;287:H767–H772.
29. du Cailar G, Ribstein J, Mimran A. Dietary sodium and target organ damage in essential hypertension. *Am J Hypertens*. 2002;15:222–229.
30. du Cailar G, Ribstein J, Grolleau R, Mimran A. Influence of sodium intake on left ventricular structure in untreated essential hypertensives. *J Hypertens Suppl*. 1989;7:S258–S259.
31. Leenen FH, Yuan B. Dietary-sodium-induced cardiac remodeling in spontaneously hypertensive rat versus Wistar-Kyoto rat. *J Hypertens*. 1998;16:885–892.
32. Doi R, Masuyama T, Yamamoto K, et al. Development of different phenotypes of hypertensive heart failure: systolic versus diastolic failure in Dahl salt-sensitive rats. *J Hypertens*. 2000;18:111–120.
33. Slama M, Ahn J, Peltier M, et al. Validation of echocardiographic and Doppler indexes of left ventricular relaxation in adult hypertensive and normotensive rats. *Am J Physiol Heart Circ Physiol*. 2005;289:H1131–H1136.
34. Musiari L, Ceriati R, Taliani U, Montesi M, Novarini A. Early abnormalities in left ventricular diastolic function of sodium-sensitive hypertensive patients. *J Hum Hypertens*. 1999;13:711–716.
35. Brilla CG, Janicki JS, Weber KT. Impaired diastolic function and coronary reserve in genetic hypertension. Role of interstitial fibrosis and medial thickening of intramyocardial coronary arteries. *Circ Res*. 1991;69:107–115.
36. Lal A, Veinot JP, Leenen FH. Prevention of high salt diet-induced cardiac hypertrophy and fibrosis by spironolactone. *Am J Hypertens*. 2003;16:319–323.
37. Yu HC, Burrell LM, Black MJ, et al. Salt induces myocardial and renal fibrosis in normotensive and hypertensive rats. *Circulation*. 1998;98:2621–2628.
38. Nathan L, Chaudhuri G. Antioxidant and prooxidant actions of estrogens: potential physiological and clinical implications. *Semin Reprod Endocrinol*. 1998;16:309–314.
39. Mendelsohn ME, Karas RH. The protective effects of estrogen on the cardiovascular system. *N Engl J Med*. 1999;340:1801–1811.
40. Nuedling S, Karas RH, Mendelsohn ME, et al. Activation of estrogen receptor beta is a prerequisite for estrogen-dependent upregulation of nitric oxide synthases in neonatal rat cardiac myocytes. *FEBS Lett*. 2001;502:103–108.
41. Sun J, Picht E, Ginsburg KS, Bers DM, Steenbergen C, Murphy E. Hypercontractile female hearts exhibit increased S-nitrosylation of the L-type Ca2+ channel alpha1 subunit and reduced ischemia/reperfusion injury. *Circ Res*. 2006;98:403–411.

42. Barouch LA, Harrison RW, Skaf MW, et al. Nitric oxide regulates the heart by spatial confinement of nitric oxide synthase isoforms. *Nature*. 2002;416:337–339.
43. Pelzer T, Shamim A, Wolfges S, Schumann M, Neyses L. Modulation of cardiac hypertrophy by estrogens. *Adv Exp Med Biol*. 1997;432:83–89.
44. Jones SP, Bolli R. The ubiquitous role of nitric oxide in cardioprotection. *J Mol Cell Cardiol*. 2006;40:16–23.
45. Jugdutt BI. Cyclooxygenase inhibition and adverse remodeling during healing after myocardial infarction. *Circulation*. 2007;115:288–291.
46. Mercier I, Colombo F, Mader S, Calderone A. Ovarian hormones induce TGF-beta(3) and fibronectin mRNAs but exhibit a disparate action on cardiac fibroblast proliferation. *Cardiovasc Res*. 2002;53:728–739.
47. Frohlich ED, Chien Y, Sesoko S, Pegram BL. Relationship between dietary sodium intake, hemodynamics, and cardiac mass in SHR and WKY rats. *Am J Physiol*. 1993;264(1 Pt 2):R30–R34.
48. Badenhorst D, Maseko M, Tsotetsi OJ, et al. Cross-linking influences the impact of quantitative changes in myocardial collagen on cardiac stiffness and remodelling in hypertension in rats. *Cardiovasc Res*. 2003;57:632–641.
49. Fischer M, Baessler A, Schunkert H. Renin angiotensin system and gender differences in the cardiovascular system. *Cardiovasc Res*. 2002;53:672–677.
50. Dubey RK, Jackson EK. Estrogen-induced cardiorenal protection: potential cellular, biochemical, and molecular mechanisms. *Am J Physiol Renal Physiol*. 2001;280:F365–F388.
51. Radin MJ, Holycross BJ, Sharkey LC, Shiry L, McCune SA. Gender modulates activation of renin-angiotensin and endothelin systems in hypertension and heart failure. *J Appl Physiol*. 2002;92:935–940.
52. Okuniewski R, Davis EA, Jarrott B, Widdop RE. A comparison of the development of renal hypertension in male and female rats. *Clin Sci (Lond)*. 1998;95:445–451.
53. Sharkey LC, Holycross BJ, Park S, et al. Effect of ovariectomy and estrogen replacement on cardiovascular disease in heart failure-prone SHHF/Mcc- fa cp rats. *J Mol Cell Cardiol*. 1999;31:1527–1537.
54. Silvestre JS, Heymes C, Oubenaissa A, et al. Activation of cardiac aldosterone production in rat myocardial infarction: effect of angiotensin II receptor blockade and role in cardiac fibrosis. *Circulation*. 1999;99: 2694–2701.
55. Vasan RS, Evans JC, Benjamin EJ, et al. Relations of serum aldosterone to cardiac structure: gender-related differences in the Framingham Heart Study. *Hypertension*. 2004;43:957–962.
56. Harvey BJ, Condliffe S, Doolan CM. Sex and salt hormones: rapid effects in epithelia. *News Physiol Sci*. 2001;16:174–177.
57. Takeda Y, Yoneda T, Demura M, Miyamori I, Mabuchi H. Sodium-induced cardiac aldosterone synthesis causes cardiac hypertrophy. *Endocrinology*. 2000;141:1901–1904.
58. Tallant EA, Ferrario CM, Gallagher PE. Angiotensin-(1-7) inhibits growth of cardiac myocytes through activation of the mas receptor. *Am J Physiol Heart Circ Physiol*. 2005;289:H1560–H1566.
59. Roongsritong C, Sutthiwan P, Bradley J, Simoni J, Power S, Meyerrose GE. Spironolactone improves diastolic function in the elderly. *Clin Cardiol*. 2005;28:484–487.
60. Daniel KR, Wells G, Gray B, Stewart KP, Kitzman DW. The effect of spironolactone on exercise tolerance and quality of life in elderly women with diastolic heart failure. *Am J Geriatr Cardiol*. 2003;12:131.
61. Izawa H, Murohara T, Nagata K, et al. Mineralocorticoid receptor antagonism ameliorates left ventricular diastolic dysfunction and myocardial fibrosis in mildly symptomatic patients with idiopathic dilated cardiomyopathy: a pilot study. *Circulation*. 2005;112:2940–2945.
62. Nishimura RA, Tajik AJ. Evaluation of diastolic filling of left ventricle in health and disease: Doppler echocardiography is the clinician's Rosetta stone. *J Am Coll Cardiol*. 1997;30:8–18.
63. Garcia MJ, Thomas JD, Klein AL. New Doppler echocardiographic applications for the study of diastolic function. *J Am Coll Cardiol*. 1998;32:865–875.
64. Ommen SR, Nishimura RA, Appleton CP, et al. Clinical utility of Doppler echocardiography and tissue Doppler imaging in the estimation of left ventricular filling pressures: a comparative simultaneous Doppler-catheterization study. *Circulation*. 2000;102:1788–1794.
65. Oki T, Tabata T, Yamada H, et al. Clinical application of pulsed Doppler tissue imaging for assessing abnormal left ventricular relaxation. *Am J Cardiol*. 1997;79:921–928.
66. Slama M, Ahn J, Peltier M, et al. Validation of echocardiographic and Doppler indexes of left ventricular relaxation in adult hypertensive and normotensive rats. *Am J Physiol Heart Circ Physiol*. 2005;289: H1131–H1136.
67. Chung CS, Kovacs SJ. Consequences of increasing heart rate on deceleration time, the velocity-time integral, and E/A. *Am J Cardiol*. 2006;97:130–136.
68. Appleton CP. Influence of incremental changes in heart rate on mitral flow velocity: assessment in lightly sedated, conscious dogs. *J Am Coll Cardiol*. 1991;17:227–236.
69. Nagueh SF, Mikati I, Kopelen HA, Middleton KJ, Quinones MA, Zoghbi WA. Doppler estimation of left ventricular filling pressure in sinus tachycardia. A new application of tissue Doppler imaging. *Circulation*. 1998;98:1644–1650.
70. Nagueh SF, Middleton KJ, Kopelen HA, Zoghbi WA, Quinones MA. Doppler tissue imaging: a noninvasive technique for evaluation of left ventricular relaxation and estimation of filling pressures. *J Am Coll Cardiol*. 1997;30:1527–1533.
71. Prunier F, Gaertner R, Louedec L, Michel JB, Mercadier JJ, Escoubet B. Doppler echocardiographic estimation of left ventricular end-diastolic pressure after MI in rats. *Am J Physiol Heart Circ Physiol*. 2002;283:H346–H352.
72. Powell BD, Redfield MM, Bybee KA, Freeman WK, Rihal CS. Association of obesity with left ventricular remodeling and diastolic dysfunction in patients without coronary artery disease. *Am J Cardiol*. 2006;98:116–120.

Received April 11, 2007
Accepted August 27, 2007
Decision Editor: Huber R. Warner, PhD